論文 / 著書情報
Article / Book Information

Title	Efficient organo-photocatalysis system of an n-type perylene derivative/p-type cobalt phthalocyanine bilayer for the production of molecular hydrogen from hydrazine
Authors	Toshiyuki Abe, Yoshinori Tanno, Naohito Taira, Keiji Nagai
Citation	RSC Advnces, Vol. 5, No. 12, pp. 46325-46329
Pub. date	2015, 5
URL	http://pubs.rsc.org/en/content/articlelanding/2015/ra/c5ra03842a

RSC Advances

COMMUNICATION

View Article Online
View Journal | View Issue

Cite this: *RSC Adv.*, 2015, **5**, 46325

Received 5th March 2015
Accepted 8th May 2015

DOI: 10.1039/c5ra03842a

www.rsc.org/advances

Efficient organo-photocatalysis system of an n-type perylene derivative/p-type cobalt phthalocyanine bilayer for the production of molecular hydrogen from hydrazine†

Toshiyuki Abe,*[a] Yoshinori Tanno,[a] Naohiro Taira[a] and Keiji Nagai[b]

The stoichiometric decomposition of hydrazine (N_2H_4) into N_2 and H_2 was observed to occur efficiently in a photocatalysis system of an organic p–n bilayer. The primary feature of the present system is that the entire visible-light energy spectrum can be utilised for N_2H_4 decomposition. Furthermore, this paper presents the first demonstration of H_2 formation by the reducing power photogenerated at the n-type perylene derivative in an organic bilayer.

Introduction

Solar hydrogen has attracted attention as a potential clean energy technology for the establishment of a sustainable society and is actively being investigated in the areas of photoelectrochemistry and photocatalysis.[1,2] Ever since Honda and Fujishima reported a photoelectrochemical water-splitting system with UV-responsive TiO_2,[3] photocatalysis researchers have aimed to extend the visible-light response of catalysts to longer-wavelength regions, particularly to enhance their photocatalytic activity towards the water-splitting reaction. However, the literature contains only a few examples of photocatalysts that are capable of H_2/O_2 evolution, even in the near-infrared region;[4–7] *i.e.* the conventional photocatalysts of band-engineered semiconductors usually exhibit diminished activity because of band-gap reduction, which is a serious issue that needs to be addressed.

We studied and reported photocatalysis systems featuring an organic p–n bilayer in terms of H_2 evolution from H^+,[8,9] as well as the decomposition of trimethylamine, alcohol and thiol into CO_2,[10,11] thereby demonstrating novel approaches to photocatalysis. These organo-photocatalysis systems can utilise the entire visible-light energy spectrum, wherein a series of photophysical events (*i.e.* exciton formation, charge separation at a heterojunction and subsequent hole and electron conduction within p-type and n-type layers, respectively) can be induced in a manner similar to that in the corresponding photovoltaic systems.[12,13] Thus, a photocatalytic reaction can be achieved by the oxidising and reducing power generated at the surface of p-type and n-type conductors, respectively.

In this study, a photocatalysis system of a 3,4,9,10-perylenetetracarboxylic-bis-benzimidazole (PTCBI, n-type)/cobalt(II) phthalocyanine (CoPc, p-type) bilayer was applied to the decomposition of a carbon-free hydrogen storage material, *i.e.* hydrazine (N_2H_4). The literature contains only a few examples of UV-responsive TiO_2 photocatalysts that are capable of photocatalysing the decomposition of N_2H_4 into N_2 and H_2 through a four-electron transfer (*vide infra*).[14] We recently reported a novel instance of a bilayer of n-type C_{60} and p-type Zn phthalocyanine (ZnPc) photocatalytically inducing the stoichiometric decomposition of N_2H_4, particularly under visible-light irradiation;[8] however, the photocatalytic activity of the present system is twice that of our previous system (based on a comparison of the optimised photocatalysis systems). Herein, we present and discuss the details of the photocatalytic decomposition of N_2H_4 by a PTCBI/CoPc bilayer.

Experimental

The PTCBI/CoPc bilayer was prepared by vapour deposition (pressure, $<1.0 \times 10^{-3}$ Pa; deposition speed, *ca.* 0.03 nm s^{-1}), and an indium–tin oxide (ITO)-coated glass plate was used as the base material. The organic bilayer comprised a PTCBI coating on ITO and CoPc coating on top of the PTCBI layer (denoted as ITO/PTCBI/CoPc). Furthermore, a Nafion

[a]*Department of Frontier Materials Chemistry, Graduate School of Science and Technology, Hirosaki University, 3 Bunkyo-cho, Hirosaki 036-8561, Japan. E-mail: tabe@hirosaki-u.ac.jp*

[b]*Chemical Resources Laboratory, Tokyo Institute of Technology, Suzukake-dai, Midori-ku, Yokohama 226-8503, Japan*

† Electronic supplementary information (ESI) available: Experimental details, function and role of Nf as absorbent, illustration of twin-compartment cell used for photoelectrolysis experiments, cyclic voltammograms, action spectrum for photocurrents, absorption spectra of PTCBI/CoPc bilayer and single-layered CoPc, photocatalysis data for N_2H_4 decomposition with respect to film thickness of photocatalyst device of PTCBI/CoPc, light intensity, hydrazine concentration and pHs employed in compartment B. See DOI: 10.1039/c5ra03842a

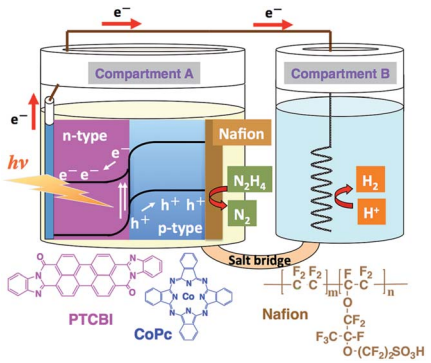

Scheme 1 Twin-compartment cell employed for photocatalysis experiments and the structures of the chemicals used in this study.

membrane (denoted as Nf) was used in combination with the bilayer, wherein (i) an alcoholic solution of Nf was cast onto the CoPc surface, followed by solvent evaporation under air, which resulted in (ii) the loading of a 1 μm thick Nf film onto that surface (the resulting photocatalytic device is abbreviated as ITO/PTCBI/CoPc/Nf).

A twin compartment cell that was separated by a salt bridge was utilised for the photocatalytic experiments (see Scheme 1). Other experimental details are provided in the ESI.†

Results and discussion

ITO/PTCBI/CoPc and ITO/PTCBI/CoPc/Nf were applied to photoanodes in an aqueous phase containing N_2H_4; this setup was used for the initial evaluation of these devices (see Fig. S1 in the ESI†). The resulting voltammograms exhibited photoanodic characteristics due to N_2H_4 oxidation (in each case, almost no electrochemical response was recorded in the absence of light). These results are consistent with those reported in our previous study, wherein the p-type material/water interface in an organic p–n bilayer induced oxidation under irradiation.[15] The aforementioned voltammetric characteristics also reveal that ITO/PTCBI/CoPc/Nf is superior to ITO/PTCBI/CoPc. This result indicates that Nf functions as an absorbent material for N_2H_4, thus producing a high surface concentration of the reactant, which ensures its efficient oxidation. Details of the function and role of Nf in the oxidation of N_2H_4 are provided in the ESI.†[8]

Photoelectrochemical decomposition of N_2H_4 at the organo-photoelectrodes was conducted under a potentiostatic condition of +0.3 V (*vs.* Ag/AgCl); a twin-compartment cell was used in this study (see Scheme S1 in the ESI†). Photoelectrolysis data related to the decomposition of N_2H_4 are presented in Table 1. In the cases of both ITO/PTCBI/CoPc/Nf (entry 1) and ITO/PTCBI/CoPc (entry 2), the stoichiometric decomposition of N_2H_4 into N_2 (oxidation product) and H_2 (reduction product) was confirmed to occur according to the following equations (eqn (1)–(3)):

$$N_2H_4 \rightarrow N_2 + 2H_2 \text{ (overall reaction)} \quad (1)$$

$$N_2H_4 \rightarrow N_2 + 4H^+ + 4e^- \text{ (oxidation)} \quad (2)$$

$$4H^+ + 4e^- \rightarrow 2H_2 \text{ (reduction)} \quad (3)$$

When the Faradaic efficiency (F.E.) of N_2 formation from N_2H_4 was estimated under the assumption of a four-electron transfer oxidation (*i.e.* eqn (2)), the F.E. values for entries 1 and 2 were calculated to be >90% (see the ESI† for the F.E. calculation procedure). The N_2H_2 intermediate may be formed through a two-electron transfer oxidation of N_2H_4 (*i.e.* $N_2H_4 \rightarrow N_2H_2 + 2H^+ + 2e^-$), followed by the further spontaneous decomposition of N_2H_2 (*i.e.* $N_2H_2 \rightarrow N_2 + H_2$).[16] However, such processes can be neglected, *i.e.* in the case of N_2 formation *via* N_2H_2, the F.E.value should be only *ca.* 50%; in addition, particularly in compartment A (see Scheme S1†), no detection of H_2 from N_2H_2 was confirmed in the present study. As supported by the aforementioned voltammograms (see Fig. S1†), the results in Table 1 also indicate that ITO/PTCBI/CoPc/Nf is the more efficient photoanode for N_2H_4 decomposition than ITO/PTCBI/CoPc. Furthermore, the results of the control experiments (*i.e.* entries 3, 4 and 5) indicate that the efficient decomposition of N_2H_4 can occur, particularly when employing the complete components of entry 1.

The photocatalytic decomposition of N_2H_4 was conducted in a system containing ITO/PTCBI/CoPc/Nf (oxidation site) and Pt wire (reduction site) (see Scheme 1). The results are listed in Table 2, which includes the results for the control experiments. Stoichiometric N_2H_4 decomposition was observed to occur in the constructed photocatalysis system (*i.e.* entry 1). In the

Table 1 Results of photoelectrolysis in the presence of hydrazine[a]

System	N_2 evolved/μL (compartment A)	H_2 evolved/μL (compartment B)	Note
Entry[b] 1	53.1	115.8	Full conditions
Entry[c] 2	38.7	80.2	Without Nf
Entry[c] 3	1.72	0	Without applied potential[d]
Entry[c] 4	0	0	Without irradiation
Entry[c] 5	0	0	In the absence of N_2H_4

[a] ITO/PTCBI/CoPc/Nf was used as the photoanode, except in the case of entry 2. [b] Film thickness: PTCBI = 200 nm, CoPc = 150 nm, Nf = 1 μm; effective area (*i.e.* geometrical area) of the photoelectrode: 1 cm^2; electrolyte solution in compartment A, 5 mM N_2H_4 (pH = 11); electrolyte solution in compartment B, H_3PO_4 (pH = 2); applied potential, +0.3 V *vs.* Ag/AgCl (satd.); light intensity, ~70 mW cm^{-2}; irradiation direction, back side of the ITO-coated face; electrolysis time, 1 h. [c] Each potentiostatic electrolysis experiment was performed under conditions similar to those used for ITO/PTCBI/CoPc/Nf (*i.e.* entry 1). [d] Irradiation of ITO/PTCBI/CoPc/Nf in compartment A was conducted in an open circuit.

control experiment, the photocatalytic decomposition of N_2H_4 was conducted in the presence of O_2 (electron acceptor), wherein only compartment B was left under aerobic conditions (*i.e.* entry 2). A comparison of the results for entry 2 with those for entry 1 revealed that the amount of N_2 evolved is almost invariable. The similarity of these results indicates that the rate-limiting oxidation of N_2H_4 can proceed at ITO/PTCBI/CoPc/Nf. The Nf absorbent resulted in an increase in the surface concentration of N_2H_4 (*vide supra*); thus, its use can lead to an enhancement of the rate-determining reaction. Furthermore, the lack of components in entry 1 in Table 2 for the experimental results of the negative control experiments (*i.e.* entries 3, 4 and 5) indicates inactivity towards N_2H_4 decomposition.

The factors affecting the photocatalysis of N_2H_4 decomposition, specifically, the thickness of the film employed (Fig. S2 in the ESI†), the light intensity (Fig. S3 in the ESI†) and the N_2H_4 concentration in compartment A (Fig. S4 in the ESI†), were examined. These results demonstrate that the conditions listed in entry 1 in Table 2 are the most appropriate conditions for the operation of the present photocatalysis system.

ITO/PTCBI/CoPc/Nf was also used in a prolonged photocatalysis study. This study was conducted under the aforementioned optimum conditions, except that the concentration of N_2H_4 was 10 mM. The amounts of N_2 and H_2 evolved after 12 h of irradiation (N_2 amount, 265.7 μL; H_2 amount, 548.4 μL) were almost proportional to those after 1 h of irradiation (N_2 amount, 22.3 μL; H_2 amount, 45.8 μL), indicating stable performance of the present photocatalysis system.

External quantum efficiency (EQE) was estimated on the basis of the amount of H_2 evolved (see the ESI† for the EQE calculation procedure), and the decomposition of N_2H_4 photocatalysed by ITO/PTCBI/CoPc/Nf under irradiation by monochromatic light was studied. Fig. 1 shows the relation between the EQE values and radiation wavelength; the resulting EQE values are consistent with the absorption spectrum of the PTCBI monolayer (Fig. 1) rather than with the spectrum of the PTCBI/CoPc bilayer (Fig. S5 in the ESI†). Moreover, N_2H_4 decomposition was induced over the entire visible-light wavelength region of $\lambda < 750$ nm. Such action spectral characteristics, which originate from the sole absorption of PTCBI in an organic p–n bilayer, have been reported by authors.[15,17,18] These details are discussed in the following paragraph, along with the mechanism of N_2H_4 decomposition.

The photocatalysis system of ITO/PTCBI/CoPc/Nf is discussed with respect to the N_2H_4 decomposition mechanism. A schematic for the present N_2H_4 decomposition is presented in Scheme 2. The photocatalytic function of the PTCBI/CoPc bilayer originates in the absorption of visible light by PTCBI (see Fig. 1 and S1†), thus resulting in the generation of oxidising power at the CoPc surface *via* a series of photophysical events within the p–n bilayer (see Introduction). An exciton, which is photogenerated within the PTCBI layer, can consequently undergo charge separation into electrons and holes at the heterojunction, followed by carrier conduction through the PTCBI and CoPc layers. In other words, the CoPc layer needs to transport hole carriers towards the N_2H_4 oxidation occurring at the phthalocyanine surface when the visible-light absorption of CoPc cannot participate in carrier generation (refer to a supporting result in Fig. S6 in the ESI†). The formal potential of $CoPc^+$/CoPc (estimated to be +0.68 V *vs.* Ag/AgCl from ref. 19 and 20) is more positive than that of N_2/N_2H_4 (−1.18 V (at pH = 11)

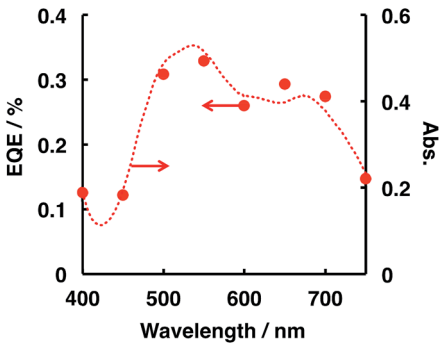

Fig. 1 Dependence of the EQE value (closed circles) on the incident wavelength in the ITO/PTCBI/CoPc/Nf and Pt wire photocatalysis system and the absorption spectrum (dashed line) of the PTCBI single layer. The conditions for entry 1 in Table 2 were used for the EQE measurements, except that monochromatic light was used. The irradiated intensity for the photocatalytic device was 0.83 mW cm^{-2}.

Table 2 Results of photocatalytic N_2H_4 decomposition in the photocatalysis system of ITO/PTCBI/CoPc/Nf and a Pt wire (see Scheme 1)[a]

System	N_2 evolved/μL (compartment A)	H_2 evolved/μL (compartment B)	Note
Entry[b] 1	20.5	41.1	Full conditions
Entry[c] 2	18.6	—	Aerobic atmosphere in compartment B
Entry[c] 3	1.72	0	No connection between ITO/PTCBI/CoPc/Nf and Pt wire
Entry[c] 4	0	0	Without irradiation
Entry[c] 5	0	0	In the absence of N_2H_4
Entry[d] 6	10.7	20.4	Data for N_2H_4 decomposition in C_{60}/ZnPc photocatalysis system (ref. 8)

[a] These experiments were conducted under a greater chemical bias between the compartments compared to those listed in Table 1. [b] Film thickness: PTCBI = 200 nm, CoPc = 150 nm, Nf = 1 μm; effective area (*i.e.* geometrical area) of the photocatalytic device, 1 cm^2; electrolyte solution in compartment A, 5 mM N_2H_4 (pH = 11); electrolyte solution in compartment B, H_3PO_4 (pH = 0); light intensity, ~70 mW cm^{-2}; irradiation direction, back side of the ITO-coated face; irradiation time, 1 h. [c] Controlled experiments were performed under conditions similar to those for entry 1. [d] The experimental conditions were the same as those listed for entry 1 in this table, except that a photocatalyst device of 200 nm C_{60}, 150 nm ZnPc and 1 μm Nf was used.

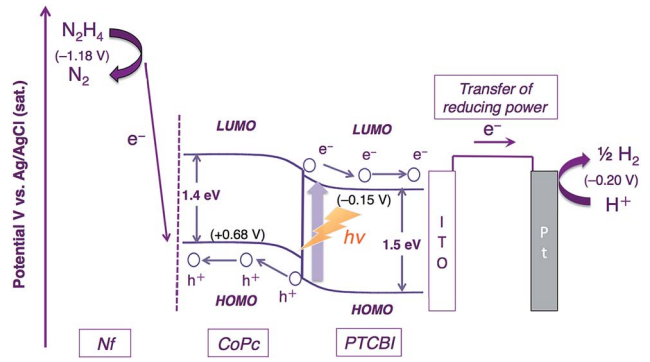

Scheme 2 Decomposition of N_2H_4 in the photocatalysis system of ITO/PTCBI/CoPc/Nf and a Pt wire.

vs. Ag/AgCl);[21] thus, in compartment A, the photocatalytic oxidation of N_2H_4 into N_2 is reasonably assumed to occur at the CoPc surface. The reducing power photogenerated at PTCBI is transferred to the Pt wire (*i.e.* co-catalyst for H_2 evolution) in compartment B where the reduction of H^+ into H_2 can occur; notably, however, the formal potential of PTCBI/PTCBI$^-$ (*i.e.* −0.15 V *vs.* Ag/AgCl, as estimated on the basis of the data from ref. 22–24) is very similar to that of H^+/H_2 (*i.e.* −0.20 V (at pH = 0) *vs.* Ag/AgCl). To gain insight into the process of H_2 formation induced by PTCBI$^-$, we conducted a separate experiment to examine the relation between the amount of H_2 evolved and pH in compartment B. As shown in Fig. S7 in the ESI,† decreasing amounts of H_2 were formed with increasing pH. This result may indicate that the PTCBI/PTCBI$^-$ potential is independent of pH, thus leading to a shortage of reducing power for H_2 evolution at a high pH (*i.e.* the difference between the PTCBI/PTCBI$^-$ and H^+/H_2 potentials is enhanced by an increase in pH level). The magnitude of the steady concentration of electrons at the Pt wire is associated with the magnitude of reducing power for H_2 formation; *i.e.* efficient H_2 evolution at pH = 0 is attributed to an effective gain in reducing power, which is based on the locally concentrated electrons.

Conclusions

In the present study, we demonstrated a novel photocatalysis system featuring a PTCBI/CoPc bilayer, which led to the stoichiometric decomposition of N_2H_4 into N_2 and H_2 over the complete visible-light wavelength range (λ < 750 nm). Furthermore, this study included the first instance of H_2 evolution that originates from the reducing power of PTCBI (*i.e.* PTCBI$^-$). We recently reported an optimised photocatalysis system of an n-type C_{60}/p-type ZnPc bilayer for N_2H_4 decomposition;[8] however, the photocatalytic activity of the present system is double that of the C_{60}/ZnPc system (see entry 6 in Table 2). A large built-in potential at the heterojunction can lead to a high carrier concentration, which is critical to the rate-limiting step in the photocatalytic reaction. However, the built-in potentials in both systems were constant (according to a previous procedure,[18] the potential in each system was estimated to be *ca.* 400 mV). Although the details are currently unclear, the more efficient activity in the PTCBI/CoPc system is speculated to originate from the higher steady concentration of holes for the rate-limiting N_2H_4 oxidation. We first realised and clarified the instance of C_{60} (n-type) participating in H_2 formation,[25] and in the current study, revealed that PTCBI is also an n-type organic material that is capable of H_2 generation. Organophotocatalysts have an advanced characteristic in the entire visible-light spectrum available for photocatalyzed reactions. The development of such organophotocatalysts is expected to open a path to the large-scale production of solar hydrogen. Towards this end, materials and active structures with p–n bilayers based on the abundant varieties of organic semiconductors must be developed in order to realise efficient photocatalysis.

Acknowledgements

This work was partly supported by a grant from Hirosaki University Institutional Research and a Grant-in-Aid for Scientific Research on innovative areas (no. 25107505) from the Ministry of Education, Culture, Sports, Science and Technology, Japan (T.A.).

References

1 M. Higashi, K. Domen and R. Abe, *J. Am. Chem. Soc.*, 2013, **135**, 10238.
2 Y. P. Xie, Z. B. Yu, G. Liu, X. L. Ma and H.-M. Cheng, *Energy Environ. Sci.*, 2014, **7**, 1895.
3 A. Fujishima and K. Honda, *Nature*, 1972, **238**, 37.
4 Y. Zhao, B. Li, Q. Wang, W. Gao, C. J. Wang, M. Wei, D. G. Evans, X. Duan and D. O'Hare, *Chem. Sci.*, 2014, **5**, 951.
5 R. Abe, K. Shinmei, N. Koumura, K. Hara and B. Ohtani, *J. Am. Chem. Soc.*, 2013, **135**, 16872.
6 H. Kaga, K. Saito and A. Kudo, *Chem. Commun.*, 2010, **46**, 3779.
7 O. Game, U. Singh, A. A. Gupta, A. Suryawanshi, A. Banpurkar and S. Ogale, *J. Mater. Chem.*, 2012, **22**, 17302.
8 T. Abe, N. Taira, Y. Tanno, Y. Kikuchi and K. Nagai, *Chem. Commun.*, 2014, **50**, 1950.
9 T. Abe, J. Chiba, M. Ishidoya and K. Nagai, *RSC Adv.*, 2012, **2**, 7992.
10 K. Nagai, T. Abe, Y. Kaneyasu, Y. Yasuda, I. Kimishima, T. Iyoda and H. Imaya, *ChemSusChem*, 2011, **4**, 727.
11 S. Zhang, A. Prabhakarn, T. Abe, T. Iyoda and K. Nagai, *J. Photochem. Photobiol., A*, 2012, **244**, 18.
12 P. Peumans, S. Uchida and S. R. Forrest, *Nature*, 2003, **425**, 158.
13 K. Suemori, T. Miyata, M. Yokoyama and M. Hiramoto, *Appl. Phys. Lett.*, 2005, **86**, 063509.
14 Y. Oosawa, *J. Chem. Soc., Faraday Trans. 1*, 1984, **80**, 1507.
15 T. Abe, K. Nagai, S. Kabutomori, M. Kaneko, A. Tajiri and T. Norimatsu, *Angew. Chem., Int. Ed.*, 2006, **45**, 2778.
16 H. Yuzawa, T. Mori, H. Itoh and H. Yoshida, *J. Phys. Chem. C*, 2012, **116**, 4126.
17 T. Abe, K. Nagai, M. Kaneko, T. Okubo, K. Sekimoto, A. Tajiri and T. Norimatsu, *ChemPhysChem*, 2004, **5**, 716.

18 T. Abe, S. Miyakushi, K. Nagai and T. Norimatsu, *Phys. Chem. Chem. Phys.*, 2008, **10**, 1562.
19 J. H. Zagal, M. A. Gulppi, C. Depretz and D. Leliévre, *J. Porphyrins Phthalocyanines*, 1999, **3**, 355.
20 D. Geraldo, C. Linares, Y.-Y. Chen, S. Ureta-Zañartu and J. H. Zagal, *Electrochem. Commun.*, 2002, **4**, 182.
21 J. Sanabria-Chinchilla, K. Asazawa, T. Sakamoto, K. Yamada, H. Tanaka and P. Strasser, *J. Am. Chem. Soc.*, 2011, **133**, 5425.
22 T. Matsushima, H. Matsuo, T. Yamamoto, A. Nakao and H. Murata, *Sol. Energy Mater. Sol. Cells*, 2014, **123**, 81.
23 R. O. Loutfy and Y. C. Cheng, *J. Chem. Phys.*, 1980, **73**, 2902.
24 B. Białek, I. G. Kim and J. I. Lee, *Thin Solid Films*, 2006, **513**, 110.
25 T. Abe, S. Tobinai, N. Taira, J. Chiba, T. Itoh and K. Nagai, *J. Phys. Chem. C*, 2011, **115**, 7701.